RSC Advances

ROYAL SOCIETY OF CHEMISTRY

www.rsc.org/advances

Journal Name

RSCPublishing

ARTICLE

Gadolinium Nicotinate Clusters as Potential MRI Contrast Agents

Cite this: DOI: 10.1039/x0xx00000x

Xinping Lin,[a] Qiongqiong Zhang,[a] Jiahe Chen,[d] Xiangjian Kong,[c] Lasheng Long,[c] Cheng Wang,[b] Wenbin Lin*[,a b]

Received 00th January 2012,
Accepted 00th January 2012

DOI: 10.1039/x0xx00000x

www.rsc.org/

ABSTRACT: Three multinuclear gadolinium(III) clusters containing the nicotinate (nic) ligand, $[Gd_2(nic)_6(H_2O)_4]$ (**1**), $[Gd_4(\mu_3\text{-}OH)_4(Hnic)_5(H_2O)_{12}](ClO_4)_8{\cdot}7H_2O$ (**2**), and $[Gd_4(\mu_3\text{-}OH)_4(nic)_6(H_2O)_6]_2(ClO_4)_4{\cdot}4H_2O$ (**3**) were synthesized and characterized. Potential applications of these Gd(III) clusters as high-field magnetic resonance imaging（MRI）contrast agents were evaluated. The longitudinal relaxivities (r_1) of **1**-**3** in water at 7 T were determined to be 10.45±0.16, 9.28±0.06, and 2.04±0.29 $mM^{-1}s^{-1}$ on a per Gd ion basis, respectively. In 1% agarose solution, the r_1 values increased slightly to 10.37±0.31, 10.74±0.11, and 4.60±0.29 $mM^{-1}s^{-1}$ for **1**-**3**, respectively. The ability to tune the number of inner-sphere water molecules, cluster sizes, organic ligands, and Gd coordination modes in such Gd(III) clusters provide interesting opportunities to further enhance the MR relaxivities for potential MRI applications.

Introduction

Magnetic resonance imaging (MRI) has become one of the most important techniques in modern diagnostic medicine because of its ability to non-invasively produce three-dimensional images of biological specimens with a deep tissue penetration and at a high spatial resolution.[1] In MRI, image contrasts result from differences of water relaxation time and proton density between adjacent tissues.[2] To enhance the image contrast, Gd(III) chelates[3] are typically employed as contrast agents to reduce the longitudinal relaxation times (T_1) of water molecules. Gd(III) contrast agents effectively increase the sensitivity of MRI, allowing reliable diagnosis of diseased states that are typically not discernible in the non-contrast enhanced MR images. The effectiveness of a Gd(III) chelate as a contrast agent is determined by its ability to relax water protons, as expressed by the longitudinal relaxivity (r_1) which is the slope of the linear dependence of $1/T_1$ vs. Gd concentration in mM.[4] Clinically used Gd(III) contrast agents, such as Gd-DPTA,[5, 6] are mononuclear compounds with a tightly bound chelating ligand and one to two coordinated water molecules.[7-10] These Gd contrast agents however tend to have modest r_1 relaxivities, particularly at high magnetic field strengths. As a result, significant amounts of Gd chelates need to be administered in order to afford adequate image contrasts between normal and pathological tissues in the clinic.[11] Significant research efforts have therefore been devoted to the development of more efficient MRI contrast agents, for example, based on dendrimers[8, 12-14] and fullerenes,[15, 16] Gd_2O_3 nanoparticles,[17, 18] nanoscale metal-organic frameworks[19-22], and other nanoparticles containing a high density of Gd chelates, in the past few years.

Metal clusters have attracted considerable attention in coordination and materials chemistry, and can be prepared by modular and metal-directed self-assembly methods.[23-29] Many of these large yet molecular species[30-35] possess beautiful structures as well as interesting optical and magnetic properties. Some of these metal clusters have potential applications as MRI contrast agents. For example, Pan and co-workers described that Mn_{12}-acetate $[Mn^{III/IV}_{12}O_{12}(CH_3CO_2)_{16}(H_2O)_4]$ could be coated with a polymeric shell via ligand-exchange to afford contrast agents with large r_1 and r_2 relaxivities of 5.2±0.12 $mM^{-1}s^{-1}$ and 10.7±0.24 at 1.5T, respectively.[36] Duan et al. reported the use of hexanuclear gadolinium-based octahedron (Gd-PT1) as selective MRI contrast agents for detecting glucosamine and observed enhanced r_1 relativity (64.8 $mM^{-1}s^{-1}$ on per a Gd ion basis, 400 MHZ, 298K) owing to the rigid facial bridging ligands.[25] In this work, we report the synthesis and characterization of three Gd clusters based on the nicotinate (nic) ligand, $Gd_2(nic)_6(H_2O)_4$ (**1**), $[Gd_4(\mu_3\text{-}OH)_4(Hnic)_5(H_2O)_{12}](ClO_4)_8{\cdot}7H_2O$ (**2**)[37] and $[Gd_4(\mu_3\text{-}OH)_4(nic)_6(H_2O)_6]_2(ClO_4)_4{\cdot}4H_2O$ (**3**). We further examined their MR relaxivities using a 7 T scanner, and studied the influences of the number of Gd ions and coordinated water molecules as well as the size of the clusters on their MR relaxivities (Figure 1).

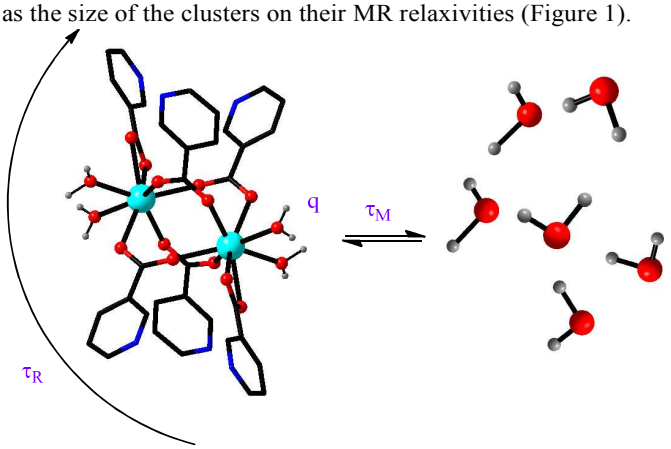

Figure 1. Molecular parameters that influence relaxivity: rotation (τ_R), water exchange (τ_M) and hydration number (q).

Experimental

Materials and General Methods. Nicotinic acid, nitric acid, gadolinium oxide, perchloric acid, sodium hydroxide, and gadolinium oxide were obtained from commercial sources. Other solvents were of reagent grade and used without further purification. Elemental analyses were performed on an Elemental Vario EL analyzer. Thermogravimetric analysis (TGA) results were obtained on a SDT Q600 Thermal Analyzer. HR-MS spectra were recorded on a Bruker En Apex ultra 7.0T FT-MS apparatus. X-ray powder diffraction patterns were obtained on a Rigaku Ultima IV XRD.

Synthesis of $Gd_2(nic)_6(H_2O)_4$ (1). The cluster **1** was prepared by a method that was modified from the procedure reported by Hong et al.[38] 10 mL of H_2O was added to a mixture of $GdCl_3{\cdot}6H_2O$ (750 mg, 2 mmol) and nicotinic acid (490 mg, 4 mmol). 650 mg of NaN_3 (10.0 mmol) was added to the solution, followed by the addition of 300 μL of 2M HNO_3. The mixture was transferred to a Teflon-lined high pressure reactor and then heated at 180 ºC for three days. The reactor was slowly cooled at 1 ºC per 10 min to room temperature, and the mixture was filtered. Colorless crystals of **1** were obtained after the solution was allowed to stand at room temperature for two days. Yield: 0.1 g (13.4%, based on nicotinic acid). Anal. Calcd for $C_{36}H_{32}Gd_2N_6O_{16}$: C, 38.6%; H, 2.86%; N, 7.50%. Found: C, 37.43%; H, 3.14%; N, 7.27%. IR (KBr): 3505(m), 1645(s), 1597(s), 1573(w), 1547 (m), 1476(m), 1433(s), 1405(s), 1195(m), 1166 (w), 1114(w), 1093(m), 1028(m), 976(w), 864m), 853(m),759(vs), 702(vs), 634(m), 566(m), 567(m) cm^{-1}. F.W. = 1119.18.

Synthesis of $[Gd_4(\mu_3\text{-}OH)_4(Hnic)_5(H_2O)_{12}](ClO_4)_8{\cdot}7H_2O$ (2). The cluster **2** was synthesized in the same way as that reported by Kong et al.[39] Block-shaped colorless crystals of **2** were obtained. Yield: 0.2 g (8.2% based on nicotinic acid). Anal. Calcd for $C_{30}Cl_8H_{67}Gd_4N_5O_{65}$: C, 14.28%; H, 2.34%; N, 2.53%. Found: C, 14.47%; H, 2.22%; N, 2.91%. IR (KBr): 3388 (m), 2861(w), 2025(w), 1643(s), 1593(s), 1417(s), 1352(w), 1305(w), 1089(s), 940(w), 835(w), 750(s), 688(s), 672(m), 627(s), 560(m) cm^{-1}. F.W. = 2450.47.

Synthesis of $[Gd_4(\mu_3\text{-}OH)_4(nic)_6(H_2O)_6]_2(ClO_4)_4{\cdot}4H_2O$ (3). The cluster **3** was synthesized by a method that was modified from the procedure reported by Kong et al .[39] Nicotinic acid (0.62 g, 5 mmol) in 5 mL of deionized water was titrated with NaOH (1.0 M) to reach a pH of 8, which was then added dropwise to the solution of 10 mL of $Gd(ClO_4)_3$ (1.0 M) that have been dropwise added a freshly NaOH (1.0 M) solution to the point of incipient but permanent precipitation at 90 °C. After stirring at 90°C for one additional hour, the resulting white epinephelos mixture was quickly filtered while hot. The mixture was allowed to stand at room temperature for two days to afford block-shaped colorless crystals. Yield: 0.13g (8.8% based on nicotinic acid). Anal. Calcd for $C_{72}H_{88}Gd_8Cl_4N_{12}O_{64}$: C, 24.4%; H, 2.48%; N, 4.74%. Found: C, 24.90%; H, 2.32%; N, 4.84%. IR (KBr): 3388(m), 1617(s), 1566(s), 1476(w), 1409(s), 1195(m), 1158 (m), 1097(m), 1030(m), 973(w), 842(m), 759(s), 698(vs), 636(m), 563(w) cm^{-1}. F.W. = 3545.34.

X-ray Crystal Structure Determination. The X-ray diffraction data of **1** and **3** were collected on Agilent Supernova with Mo-Kα radiation (λ = 0.71073 Å) at 100 K. Absorption corrections were applied by using the multiscan program CrysAlis Red. The structures were solved by direct and Fourier methods and refined by full-matrix least squares based on F_2 using the SHELX and Olex2 software. Detailed crystal data and refinement parameters are listed in Table S1.

Measurement of r_1 relaxivities. To measure the r_1 relaxivities of **1-3**, samples with different Gd(III) concentrations were dispersed in Mill-Q water or in 1% agarose solution. The Gd(III) concentrations were measured by inductively coupled plasma-mass spectrometry (ICP-MS). The samples were scanned (at 300 K) on both 0.5 T and 7 T MRI scanners. T_1-weighted MRI phantom images of the three samples are performed on a 7T MRI scanner.

Results and discussion

Synthesis. Cluster **1** was synthesized in 13.4% yield by first hydrothermally treating a mixture of nicotinic acid, $GdCl_3$, and NaN_3 in the presence of a small amount of HNO_3 followed by crystallization at room temperature over a period of two days.[38] Clusters **2** and **3** were prepared in low yield (about 8%) by first heating appropriate mixtures at 90 °C, followed by crystallization at room temperature. Such a ligand-controlled hydrolytic approach has been previously established for Gd cluster synthesis.[40, 41] The structures and compositions of **1-3** have been established by single-crystal X-ray crystallography, powder X-ray diffraction, and elemental analysis. Cluster **2** was prepared by a one-pot synthesis method whereby an aqueous solution of NaOH was added dropwise into the mixture containing both the nicotinic acid ligand and the Gd salt. In contrast, cluster **3** was obtained by a two-step procedure. The pH of the ligand aqueous solution and the lanthanide perchlorate was adjusted individually to appropriate values before they were mixed. The one-pot synthesis produced the tetranuclear cluster of $[Gd_4(\mu_3\text{-}OH)_4(Hnic)_5(H_2O)_{12}](ClO_4)_8{\cdot}7H_2O$, while the two-step synthesis afforded $[Gd_4(\mu_3\text{-}OH)_4(nic)_6(H_2O)_6]_2(ClO_4)_4{\cdot}4H_2O$. Cluster **3** slightly differs from $[Gd_4(\mu_3\text{-}OH)_4(nic)_6(H_2O)_8]_2(ClO_4)_4{\cdot}3H_2O$ which was previously described by Long et al. The pyridyl nitrogen atoms of the nic ligands in cluster **2** was protonated, while the nic ligands in cluster **3** were completely deprotonated.

X-ray Single Crystal Structures. Single-crystal X-ray diffraction analyses reveal that **1** is a neutral dinuclear compound that crystallizes in the monoclinic space group $P2_1/c$. In **1**, each Gd^{3+} ion is coordinated to eight oxygen atoms (Figure 2), with two oxygen atoms coming from a chelating nicotinic acid ligand, four oxygen atoms coming from four bridging nicotinic acid ligands, and two oxygen atoms from two water molecules.[42] Each Gd ion is thus coordinated to two water molecules in **1**. In addition, there are two crystallization water molecules for each molecule of **1** in the crystals.

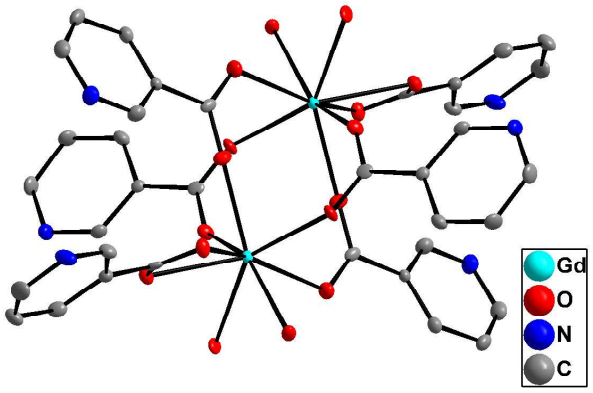

Figure 2. X-ray single-crystal structure of $[Gd_2(nic)_6(H_2O)_4]$ (**1**) with thermal ellipsoids at the 50% probability level. Hydrogen atoms are removed for clarity. Each Gd(III) ion has two coordinated water molecules.

The structure of **2** was previously reported by Kong et al.[37] Briefly, the $[Gd_4(\mu_3\text{-}OH)_4]^{8+}$ cationic core adopts a distorted cubane structure (Figure 3). Two Gd ions (Gd1 and Gd2) have two coordinated water molecules whereas two other Gd ions (Gd3 and Gd4) have four coordinated water molecules. All of the pyridyl nitrogen atoms of the nicotinate ligands in **2** are protonated to maintain charge balance.

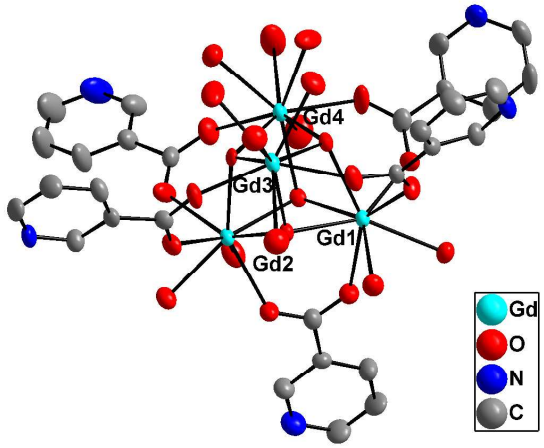

Figure 3. X-ray single-crystal structure of $[Gd_4(\mu_3\text{-}OH)_4(Hnic)_5(H_2O)_{12}](ClO_4)_8\cdot 7H_2O$ (**2**) with thermal ellipsoids at the 50% probability level. Perchlorate anions, crystallization water molecules, and hydrogen atoms are removed for clarity.

The molecular structure of **3** consists of a dimer of $[Gd_4(\mu_3\text{-}OH)_4(nic)_6(H_2O)_6]^{2+}$ as shown in Figure 4. There is an inversion center residing at the center of the dimer. The $Gd_4(\mu_3\text{-}OH)_4$ cubane core is encapsulated by six nicotinate ligands. These ligands display two different coordination modes: five of them use their carboxylate groups to bridge two Gd^{3+} ions whereas the sixth one uses its carboxylate group to bridge two Gd^{3+} ions of one $Gd_4(\mu_3\text{-}OH)_4$ cubane core and uses its pyridyl N atom to coordinate a Gd^{3+} ion in the other $Gd_4(\mu_3\text{-}OH)_4$ cubane core (as shown for Gd4 and Gd3 in Figure 4).

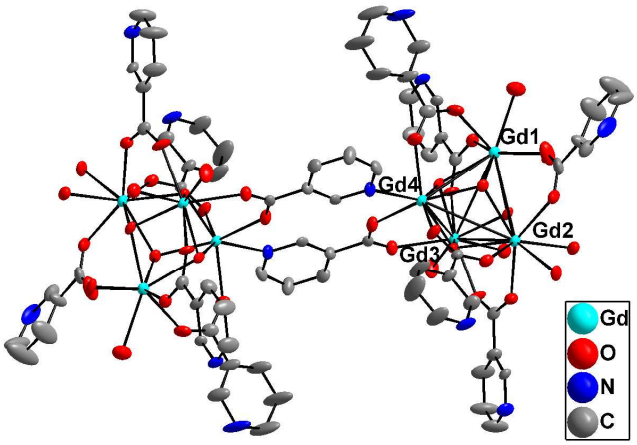

Figure 4. X-ray single-crystal structure of $[Gd_4(\mu_3\text{-}OH)_4(nic)_6(H_2O)_6]_2(ClO_4)_4\cdot 4H_2O$ (**3**) with thermal ellipsoids at the 50% probability level. Perchlorate anions and hydrogen atoms are removed for clarity.

Gd1, Gd2, and Gd3 centers in **3** are thus 8-coordinate, by binding to three oxygen atoms from the bridging nicotinate ligands, three μ_3-OH groups, and two water molecules. The Gd4 center is seven-coordinate and binds to three oxygen atoms from the bridging nicotinate ligands, three μ_3-OH groups, and one pyridyl atom of the bridging nicotinate ligand. The structure of **3** is related to, but distinct from an octanuclear Gd complex with the formula of $[Gd_4(\mu_3\text{-}OH)_4(nic)_6(H_2O)_8]_2(ClO_4)_4\cdot 3H_2O$ that was reported earlier.[37]

Characterization of Clusters 1-3 by PXRD, TGA and ESI-MS. We have used PXRD to verify the phase purity of the clusters. As shown in Figures 5a-c, the experimental PXRD patterns of **1-3** generally match the PXRD patterns that were simulated from their single crystal structures well, indicating that the bulk phase of these clusters are identical to those of the single crystals chosen for X-ray diffraction studies. We note a slight peak shift in PXRD pattern of **3** from the simulated pattern, which can be attributed to different temperature between the single crystal X-ray and PXRD experiment as well as possible partial loss of lattice solvent molecules in the powdery samples for PXRD. Indexing the PXRD pattern of **3** gives similar lattice parameters to those determined from single crystal data (Table S3, Figure S7).
Thermogravimetric analyses (TGA) were also performed on clusters **1-3**. As shown in Figure 5d, the TGA curves for **1-3** display an initial weight loss 6.4%（calcd 7.9%）for **1**, 12.5%(calcd 13.9%) for **2**, and 8.1% (calcd 9.0%) for **3** at the room temperature to 300 ℃ temperature range, which correspond to the loss of guest and coordinated water molecules. When the temperature is higher than 300 °C, clusters of **1-3** were rapidly decomposed to form Gd_2O_3 with remaining weight of 32.5% (calcd 32.4%) for **1**, 30.1%(calcd 29.6%) for **2**, and 40.0% (calcd 40.9%) for **3** at 900 ℃.
We have also tried to characterize the clusters using electrospray ionization-mass spectrometry to ensure that the clusters remain intact when they are dissolved in aqueous solutions. As shown in Figure S1, the ESI-MS spectrum (positive ion mode) of **1** gave the most intense peak at m/Z=1049.00, which corresponding to the fragment of $[Gd_2(nic)_6+H]^+$. This assignment was further confirmed by the isotopic distribution pattern of the $[Gd_2(nic)_6+H]^+$ fragment. As shown in Figure 6a and 6b, the experimental and theoretical isotopic distribution patterns match extremely well.

The ESI-MS spectra of **2** and **3** indicate that the clusters have undergone extensive fragmentation during the electrospray ionization process. We have not been able to unambiguously assign the major peaks in their ESI-MS spectra. Instead, we resorted to dynamic light scattering (DLS) to probe the species resulted from the dissolution of **2** and **3** in aqueous solutions.

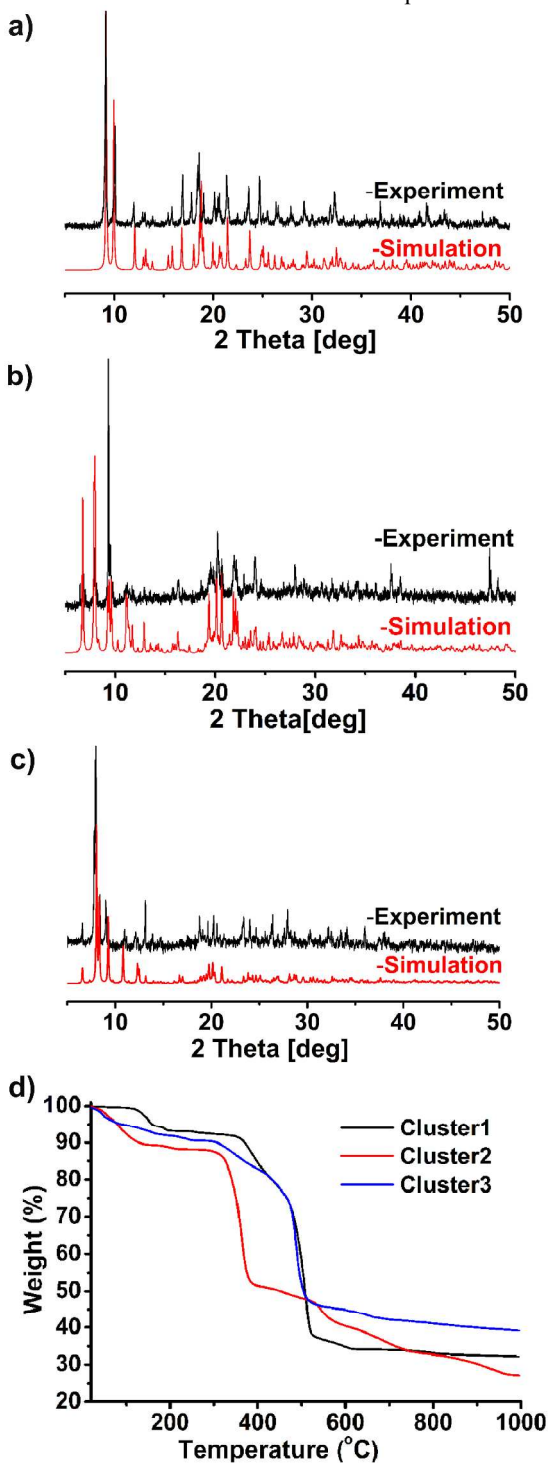

Figure 5. a-c) PXRD patterns of cluster **1** (a); cluster **2** (b), and cluster **3** (c). PXRD pattern of the as-synthesized sample (black), simulated from single-crystal structure (red). d) TGA curves for cluster **1**(black); cluster **2**(red); cluster **3**(blue).

As shown in Figure S3 and S4, DLS data indicate the presence of hydrodynamic diameter peaks centering at 0. 9 nm and 1.8 nm for **2** and **3**, respectively. These DLS hydrodynamic diameters are consistent with the molecular dimensions of **2** and **3**: the short and

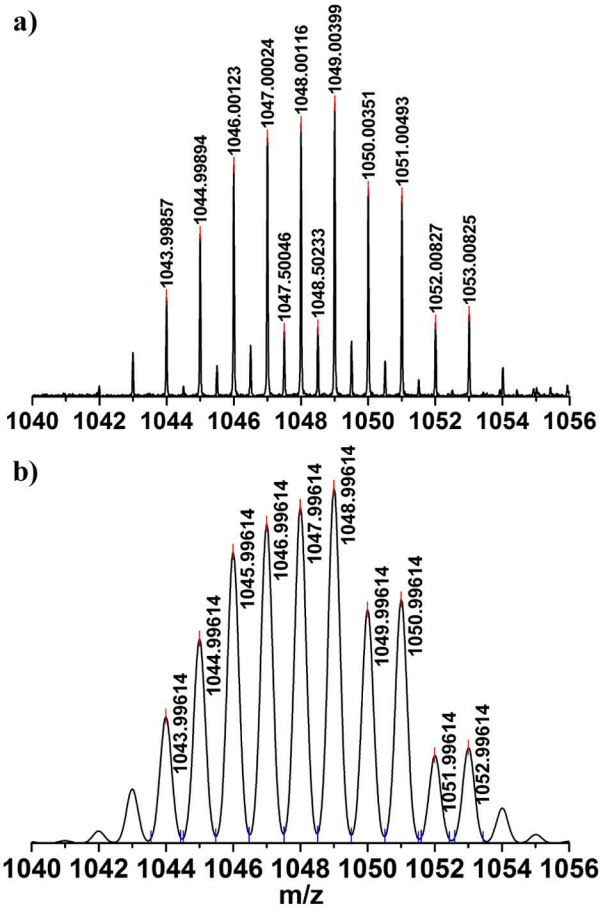

Figure 6. The measured mass spectrum (a) and simulated (b) isotopic distributions of **1** (The shorter isotope peaks at 1048.50 m/z belong to the $[Gd_4(nic)_{12}+2H]^{2+}$ which might have formed during the ionization events of the ESI-MS experiments).

long dimensions of **2** are 0.6 and 1.7 nm, respectively, and the short and long dimensions of **3** are 0.9 and 2.7 nm, respectively. The DLS data thus support the notion that clusters **2** and **3** remain intact upon dissolution in aqueous solutions.

r_1 Measurements and T_1-Weighted MRI Phantom Images. With seven unpaired electrons in each Gd ion, we expect that the synthesized Gd clusters to exhibit strong ability to relax water protons. We determined the longitudinal relaxivity (r_1) values of **1-3** at both 0.5 T and 7 T. Each type of the clusters was prepared by dissolving them in 1% agarose solution with total Gd concentrations of 0.025, 0.1, 0.2, and 0.4 mM. As shown in Figure 7a, the T_1-weighted signal intensities in a 7 T scanner increase as the Gd concentration of the clusters increase, indicating that all of the clusters have the ability to enhance MRI contrasts with T_1-weighted pulse sequences. At 7T, the r_1 values for **1-3** are 10.45±0.16, 9.28±0.06, and 2.04±0.29 $mM^{-1}\cdot s^{-1}$ in water through the linear fit in Figure 7b, respectively. In 1% agarose solution, the r_1 values increased slightly to 10.37±0.31, 10.74±0.11, and 4.60±0.29 $mM^{-1}s^{-1}$ for **1-3**, respectively. The r_1 values of the cluster **1** and **2** in 1% agarose are significantly higher than that of Gd-DTPA (r_1=3.30±0.25 $mM^{-1}\cdot s^{-1}$ at 7T) which we have determined under the same conditions. As expected, the r_1 values for **1-3** decrease as the

field strength increases; at 0.5 T, the r_1 values are 11.00±0.25, 10.08±0.22, and 2.09±0.32 $mM^{-1}\cdot s^{-1}$ for **1-3** in water, respectively (Figure S5). The two Gd clusters of the **1** and **2** show high r_1 relaxivities at 7 T, and they exhibit interesting relaxivity

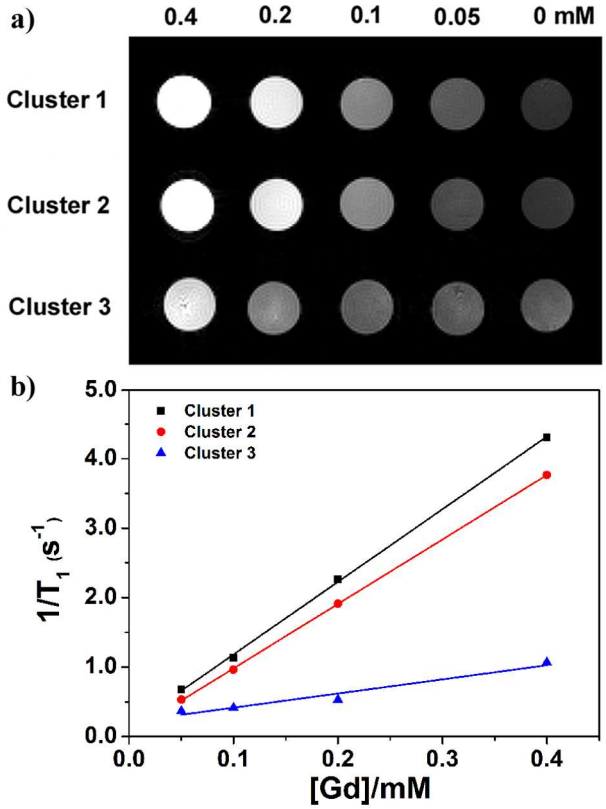

Figure 7. The phantom study (a) and relaxivity values r_1(b) of the three clusters performed on a 7 T MRI scanner.

trends due to their different coordination environments. As described in the Solomon–Bloembergen–Morgan equations, the key factors contributing to the inner-sphere relaxivity include the rotational tumbling time (τ_R), the number of inner-sphere water molecules (q), and the residence lifetime of inner-sphere water molecules (τ_m). A larger relaxivity value will result when inner-sphere water have greater access to the paramagnetic metal center (i.e., shorter τ_m) and the inner-sphere relaxivity is linearly proportional to the number of inner-sphere water molecules (q).[43] Since the molecular weights of the cluster ions range from 1119 to 3075 for **1-3**, their tumbling rates in water should be relatively fast. We do not expect that the differences in tumbling rates of these clusters will significantly influence their r_1 values. Instead, the number of coordinated water molecules and the steric hindrance around the water coordination sites for **1-3** should have significant impacts on their r_1 values. Cluster **2** has the largest average number of coordinated water molecules per Gd (q_{ave}=3), whereas cluster **3** has the smallest average number of coordinated water molecules per Gd (q_{ave}=1.5). As a result, the r_1 value for **2** is much higher than that of **3**. Although **2** has a larger average number of coordinated water molecules per Gd than **1** (q_{ave}=2), their r_1 values are essentially identical. X-ray structure comparisons indicate that the water coordination sites in **1** are more open than those in **2**, and as a result, the τ_m value for **2** should be smaller, which compensate for its smaller q_{ave} value.

Conclusions

We have prepared and characterized three gadolinium nicotinate clusters of different sizes. These Gd clusters of the cluster **1** and **2** have very high relaxivities at 7T when compared to the clinically used Gd-DTPA. Because of the ability to tune the number of inner-sphere water molecules, cluster sizes, organic ligands, and Gd coordination modes in such Gd(III) clusters, we believe that Gd clusters provide interesting opportunities for designing new multinuclear MRI contrast agents for potential biological and biomedical imaging.

Acknowledgements

The work was supported by the National Natural Science Foundation of P. R. China (21471126), the National Thousand Talents Program of P.R. China, and the 985 Program of the Chemistry and Chemical Engineering disciplines of Xiamen University. We acknowledge Ms. Zhiwei Lin for the FT-MS measurement and Ms. Ruiyun Huang for administrative help.

Notes and references

[a]Collaborative Innovation Center of Chemistry for Energy Materials, College of Chemistry and Chemical Engineering, Xiamen University, Xiamen 361005, P.R. China.
[b]Department of Chemistry, University of Chicago, 929 E 57th Street, Chicago, IL 60637, USA.
[c]State Key Laboratory of Physical Chemistry of Solid Surfaces, Department of Chemistry, College of Chemistry and Chemical Engineering, Xiamen University, Xiamen 361005, China.
[d]Department of Physics and Electronic Science, Fujian Key Laboratory of Plasma and Magnetic Resonance, Xiamen University, Xiamen 361005, China.

Electronic Supplementary Information (ESI) available: X-ray crystallography, Electrospray mass spectrum, IR spectra and DLS spectra. CCDC references 1014973 for **1** and 1014974 for **3**. See DOI: 10.1039/b000000x/

1 X. Zhang, X. Jing, T. Liu, G. Han, H. Li and C. Duan, *Inorg. Chem.*, 2012, **51**, 2325.
2 L. N. Goswami, L. Ma, S. Chakravarty, Q. Cai, S. S. Jalisatgi and M. F. Hawthorne, *Inorg. Chem.*, 2013, **52**, 1694.
3 T. Courant, V. G. Roullin, C. Cadiou, M. Callewaert, M. C. Andry, C. Portefaix, C. Hoeffel, M. C. de Goltstein, M. Port, S. Laurent, L. V. Elst, R. Muller, M. Molinari and F. Chuburu, *Angew. Chem., Int. Ed.*, 2012, **51**, 9119.
4 E. J. Werner, A. Datta, C. J. Jocher and K. N. Raymond, *Angew. Chem., Int. Ed.*, 2008, **47**, 8568.
5 DE3640708A1, 1988.
6 C. T. Williams, J. P. Stack, B. Loveday, Y. Watson and I. Isherwood, *Br. J. Radiol.*, 1988, **61**, 596.
7 D. T. Puerta, M. Botta, C. J. Jocher, E. J. Werner, S. Avedano, K. N. Raymond and S. M. Cohen, *J. Am. Chem. Soc.*, 2006, **128**, 2222.
8 P. Caravan, J. J. Ellison, T. J. McMurry and R. B. Lauffer, *Chem. Rev. (Washington, D. C.)*, 1999, **99**, 2293.
9 Z. Zhang, A. F. Kolodziej, M. T. Greenfield and P. Caravan, *Angew. Chem., Int. Ed.*, 2011, **50**, 2621.
10 J. Xu, D. G. Churchill, M. Botta and K. N. Raymond, *Inorg. Chem.*, 2004, **43**, 5492.
11 H. Ersoy and F. J. Rybicki, *J Magn Reson Imaging*, 2007, **26**, 1190.

12 E. Boros, M. Polasek, Z. Zhang and P. Caravan, *J. Am. Chem. Soc.*, 2012, **134**, 19858.
13 P. Caravan, G. Parigi, J. M. Chasse, N. J. Cloutier, J. J. Ellison, R. B. Lauffer, C. Luchinat, S. A. McDermid, M. Spiller and T. J. McMurry, *Inorg. Chem.*, 2007, **46**, 6632.
14 E. Garanger, S. A. Hilderbrand, J. T. Blois, D. E. Sosnovik, R. Weissleder and L. Josephson, *Chem. Commun. (Cambridge, U. K.)*, 2009,**29**, 4444.
15 K. B. Ghiassi, M. M. Olmstead and A. L. Balch, Dalton Trans., 2014, **43**, 7346.
16 M. Mikawa, H. Kato, M. Okumura, M. Narazaki, Y. Kanazawa, N. Miwa and H. Shinohara, Bioconjug. Chem., 2001, **12**, 510.
17 M. L. Viger, J. Sankaranarayanan, C. de Gracia Lux, M. Chan and A. Almutairi, *J. Am. Chem. Soc.*, 2013, **135**, 7847.
18 A.-A. Guay-Bégin, P. Chevallier, L. Faucher, S. Turgeon and M.-A. Fortin, *Langmuir*, 2011, **28**, 774.
19 K. M. L. Taylor, A. Jin and W. Lin, *Angew. Chem., Int. Ed.*, 2008, **47**, 7722.
20 J. Della Rocca, D. Liu and W. Lin, *Acc. Chem. Res.*, 2011, **44**, 957.
21 M. D. Rowe, C.-C. Chang, D. H. Thamm, S. L. Kraft, J. F. Harmon, A. P. Vogt, B. S. Sumerlin and S. G. Boyes, *Langmuir*, 2009, **25**, 9487.
22 W. Hatakeyama, T. J. Sanchez, M. D. Rowe, N. J. Serkova, M. W. Liberatore and S. G. Boyes, *ACS Appl. Mater. Interfaces.*, 2011, **3**, 1502.
23 M. W. Cooke and G. S. Hanan, *Chem. Soc. Rev.*, 2007, **36**, 1466.
24 X.-J. Kong, Y. Wu, L.-S. Long, L.-S. Zheng and Z. Zheng, *J. Am. Chem. Soc.*, 2009, **131**, 6918.
25 C. He, X. Wu, J. Kong, T. liu, X. Zhang and C. Duan, *Chem. Commun.*, 2012, **48**, 9290.
26 D. T. Thielemann, A. T. Wagner, E. Rösch, D. K. Kölmel, J. G. Heck, B. Rudat, M. Neumaier, C. Feldmann, U. Schepers, S. Bräse and P. W. Roesky, *J. Am. Chem. Soc.*, 2013, **135**, 7454.
27 Y.-L. Hou, G. Xiong, P.-F. Shi, R.-R. Cheng, J.-Z. Cui and B. Zhao, *Chem. Commun. (Cambridge, U. K.)*, 2013, **49**, 6066.
28 L.-X. Chang, G. Xiong, L. Wang, P. Cheng and B. Zhao, *Chem. Commun.*, 2013, **49**, 1055.
29 S. K. Langley, B. Moubaraki and K. S. Murray, *Inorg. Chem.*, 2012, **51**, 3947.
30 J. Bai, A. V. Virovets and M. Scheer, *Science*, 2003, **300**, 781.
31 T. C. Stamatatos, K. A. Abboud, W. Wernsdorfer and G. Christou, *Angew. Chem., Int. Ed.*, 2007, **46**, 884.
32 H.-H. Zou, R. Wang, Z.-L. Chen, D.-C. Liu and F.-P. Liang, *Dalton Trans.*, 2014, **43**, 2581.
33 N. M. Randell, M. U. Anwar, M. W. Drover, L. N. Dawe and L. K. Thompson, *Inorg. Chem.*, 2013, **52**, 6731.
34 J.-M. Jia, S.-J. Liu, Y. Cui, S.-D. Han, T.-L. Hu and X.-H. Bu, *Cryst. Growth Des.*, 2013, **13**, 4631.
35 F.-S. Guo, Y.-C. Chen, L.-L. Mao, W.-Q. Lin, J.-D. Leng, R. Tarasenko, M. Orendáč, J. Prokleška, V. Sechovský and M.-L. Tong, *Chem. Eur. J.*, 2013, **19**, 14876.
36 B. Kim, A. H. Schmieder, A. J. Stacy, T. A. Williams and D. Pan, *J. Am. Chem. Soc.*, 2012, **134**, 10377.
37 X.-J. Kong, L.-S. Long, L.-S. Zheng, R. Wang and Z. Zheng, *Inorg. Chem.*, 2009, **48**, 3268.
38 M. Wu, F. Jiang, X. Kong, D. Yuan, L. Long, S. A. Al-Thabaiti and M. Hong, *Chem Sci.*, 2013, **4**, 3104.
39 X.-J. Kong, L.-S. Long, L.-S. Zheng, R. Wang and Z. Zheng, *Inorg. Chem.*, 2009, **48**, 3268.
40 R. Wang, Z. Zheng, T. Jin and R. J. Staples, *Angew. Chem., Int. Ed.*, 1999, **38**, 1813.
41 R. Wang, H. Liu, M. D. Carducci, T. Jin, C. Zheng and Z. Zheng, *Inorg. Chem.*, 2001, **40**, 2743.
42 W. Chen and S. Fukuzumi, *Inorg. Chem.*, 2009, **48**, 3800.
43 E. L. Que and C. J. Chang, *Chem. Soc. Rev.*, 2010, **39**, 51.

TOC Graphic: